ASME Journal of Mechanical Design
Online journal at:
https://asmedigitalcollection.asme.org/mechanicaldesign

Weifei Hu[1]
Mem. ASME
State Key Laboratory of Fluid Power and Mechatronic Systems,
Zhejiang University,
Hangzhou 310058, China
e-mail: weifeihu@zju.edu.cn

Jiquan Yan
School of Mechanical Engineering,
Zhejiang University,
Hangzhou 310058, China
e-mail: jiquanyan@zju.edu.cn

Feng Zhao
State Key Laboratory of Fluid Power and Mechatronic Systems,
Zhejiang University,
Hangzhou 310058, China
e-mail: feng_zhao@zju.edu.cn

Chen Jiang
School of Mechanical Science and Engineering,
Huazhong University of Science and Technology,
Wuhan 430074, China
e-mail: chenjiang@hust.edu.cn

Hongwei Liu
State Key Laboratory of Fluid Power and Mechatronic Systems,
Zhejiang University,
Hangzhou 310058, China
e-mail: lhwei@zju.edu.cn

Hyunkyoo Cho
Department of Mechanical Engineering,
Mokpo National University,
Muan-gun, Jeollanam-do 58554,
Republic of Korea
e-mail: hyunkcho@mokpo.ac.kr

Ikjin Lee
Department of Mechanical Engineering,
Korea Advanced Institute of Science and Technology,
Daejeon 34141, Republic of Korea
e-mail: ikjin.lee@kaist.ac.kr

Surrogate-Based Time-Dependent Reliability Analysis for a Digital Twin

A mature digital twin (DT) is supposed to enable engineers to accurately evaluate the real-time reliability of a complex engineering system. However, in practical engineering problems, reliability analysis (RA) often involves nonlinear, implicit, and computationally expensive relationships between the performance and uncertain parameters, which makes it very challenging to conduct time-dependent reliability analysis (TRA) instantly and accurately for a DT. This article proposes a new surrogate-based time-dependent reliability analysis (STRA) method for a DT, specifically making the following three contributions: (i) the number of discrete time nodes used to convert the stochastic processes into a series of random variables in the expansion optimal linear estimation process is dynamically selected, leading to a good tradeoff between the accurate representation of stochastic processes and fast reliability evaluation; (ii) based on Voronoi partition sampling and a modified leave-one-out cross-validation procedure, multiple sensitive subdomains in each iteration are selected simultaneously to guide adaptive sampling at the insufficiently fitted vicinity of the limit state function, which helps accurately calculate the probability of failure and reduce the number of design-of-experiment (DoE) samples; and (iii) an improved weighted expected feasibility function is proposed considering the importance of each sample and the sensitivity of the subdomain to which it belongs, which further improves the sampling efficiency. The proposed STRA method is applied to the TRA of a numerical model, a corroded beam structure, and a cutterhead of a tunnel boring machine to demonstrate its effectiveness for realistic DT applications.
[DOI: 10.1115/1.4062668]

Keywords: time-dependent reliability analysis, surrogate model, digital twin, expansion optimal linear estimation, adaptive sampling strategy, kriging, metamodeling, reliability in design

1 Introduction

Real-time and accurate time-dependent reliability analysis (TRA) should be one of the key characteristics of a mature digital twin (DT), as it is supposed to be able to reflect the operational condition and reliability of a complex engineering system throughout its

[1]Corresponding author.
Contributed by the Design Automation Committee of ASME for publication in the Journal of Mechanical Design. Manuscript received January 27, 2023; final manuscript received May 23, 2023; published online July 18, 2023. Assoc. Editor: Pingfeng Wang.

lifecycle [1–5]. However, TRA of practical engineering systems often involves nonlinear, implicit, and computationally expensive relationships between the performance and uncertain parameters (e.g., random variables and stochastic processes), which makes it very challenging to conduct TRA instantly and accurately for a DT.

Recently, various TRA methods for real-world engineering problems have been widely investigated to address the efficiency and accuracy challenges. They can be mainly classified into outcrossing rate methods and extreme value methods. Methods of the former type calculate the probability of encountering the first outcrossing event within a predefined time interval. Based on the assumption that the outcrossing events are independent, the PHI2 method was proposed by using the first-order reliability method [6]. Later, an improved PHI2 method (PHI2+) was proposed to stabilize the PHI2 method [7]. However, these methods may produce large errors when the outcrossing events are strongly dependent. To describe the dependence among different outcrossing events, the Markov process model [8] and joint outcrossing rate [9] were utilized. Jiang et al. [10] presented an outcrossing rate model that can efficiently handle TRA for system reliability problems. Although many improvements have been proposed, the time-consuming calculation and dependence assumptions still limit the applicability of outcrossing rate methods to DTs.

Methods of the latter type calculate the probability that the extreme value of the performance exceeds the specified performance threshold of an engineering system. Several surrogate models, including polynomial response surface [11,12], polynomial chaos expansion [13], support vector machine [14], and kriging [15] models, have been used in extreme value methods, which are named surrogate-based time-dependent reliability analysis (STRA) methods in this paper. Extreme response surrogate methods, such as the nested extreme response surface method [16] and the mixed efficient global optimization method [17], aim at constructing an extreme response surface with respect to time. Li et al. [18] proposed the idea of equivalent extreme value event and combined the probability density evolution method to achieve the reliability evaluation of structures. Multiple kriging models at discretized time nodes were built by Wang and Chen [19]. Wu et al. [20] developed a time-dependent system reliability method that is extended from the component time-dependent reliability method using the envelope method and second-order reliability method. Li et al. [21] proposed the instantaneous response surface (*t*-IRS) method for constructing one instantaneous response surrogate model, leading to a great reduction in the computational load. However, these methods still require a large number of performance evaluations, which hinders their application to DTs.

As a real-time virtual representation of a real-world physical system, a DT of a complex engineering system is expected to serve as an indistinguishable digital counterpart for practical purposes, such as system simulation, design, integration, testing, monitoring, and maintenance [22,23]. Hence, a mature high-fidelity DT is supposed to enable the accurate and efficient real-time and in situ TRA of a complex engineering system [24], which poses significant new challenges for the aforementioned traditional TRA methods:

(1) Surrogate models used for STRA should be quickly generated for ready application in reliability analyses under various random variables and stochastic processes. If the generation of a surrogate model for STRA requires a large number of design-of-experiment (DoE) samples, the generation of these DoE samples will cost a significant amount of time, which will prevent real-time reliability analysis (RA) using a DT under realistic working conditions.
(2) After the surrogate model is established, the STRA process should be instantly conducted for real-time reliability evaluation. If the STRA process requires a significant amount of computation time, the calculated reliability or failure probability will inherently have a time delay, which is also not suitable for a DT.
(3) The accuracy of the STRA results lays the foundation for the high credibility of a DT. Obviously, if the STRA cannot accurately predict the failure probability, it cannot satisfy the requirement that the DT accurately reflects the reliability of a complex engineering system.

To efficiently generate a surrogate model for TRA, an adaptive sampling strategy is often used to reduce the number of DoE samples. For instance, Echard et al. [25] first proposed the idea of importance sampling and introduced the importance density distribution function to improve the sampling efficiency. On this basis, Xiao et al. [26] proposed a method of stratified importance sampling to further improve the sampling efficiency. Yang et al. [27] proposed a new active learning function called the expected system improvement for system reliability analysis. To guide the choice of samples, Jiang et al. [28] proposed a failure-pursuing sampling framework with sensitive Voronoi cells. However, this method focuses only on the most sensitive cell and may ignore other vital information and prematurely terminate the iterative sampling process. Peng et al. [29] proposed an adaptive kriging model of failure probability considering the uncertainties of distribution parameters. After constructing a surrogate model, Monte Carlo simulation (MCS) is often used to calculate the probability of failure. Obviously, the number of time nodes that are used to discretize a stochastic process into random variables before the MCS will affect the computation time of the TRA. Hence, for real-time reliability analysis applicable to a DT, the number of discretized time nodes should be as small as possible, which has not been considered in existing STRA methods.

To improve the accuracy of the TRA results, the estimation error of the failure probability has been directly considered when constructing the surrogate model. For instance, Jiang et al. proposed a real-time estimation error-guided active learning kriging method (REAL), which computes the incorrect-classification probability [30]. Song et al. proposed an estimation variance reduction-guided adaptive kriging method considering the estimation variance of the time-variant failure probability [31]. In addition, expansion optimal linear estimation (EOLE) has often been used to convert the time-dependent reliability analysis to a time-independent reliability analysis [32]. However, the EOLE method ignores the influence of the number of discretized time nodes on the approximation error of stochastic processes, which affects the accuracy of the TRA results.

To address the aforementioned challenges, this article proposes a new STRA method for a DT, making the following key contributions:

(1) The number of discrete time nodes used to convert the stochastic processes into a series of random variables in the EOLE is dynamically selected, leading to a good tradeoff between the accurate representation of the stochastic processes and fast reliability evaluation.
(2) Based on Voronoi partition sampling [33] and a modified leave-one-out (LOO) cross-validation procedure, multiple sensitive subdomains in each iteration are selected simultaneously to guide the adaptive sampling in the insufficiently fitted vicinity of the limit state function (LSF), which helps accurately calculate the probability of failure and reduce the number of design-of-experiment (DoE) samples.
(3) An improved weighted expected feasibility function (WEFF) is proposed considering the importance of each sample and the sensitivity of the subdomain to which it belongs, which further improves the sampling efficiency.

The remainder of this article is organized as follows. Section 2 reviews the background of TRA and its role in a DT framework. Section 3 presents the proposed STRA method in detail. Section 4 uses three examples to show the performance of the proposed STRA method. Section 5 presents the conclusions of the article.

2 Time-Dependent Reliability Analysis in a Digital Twin

A DT needs to accurately assess the reliability of equipment or systems and predict the probability of failure over a period of time. Specifically, time-dependent reliability analysis in a DT refers to calculating the probability of a structure performing its expected function within a given time interval based on the DT's real-time measured data. The fundamentals of TRA and the kriging model are briefly explained in this section.

2.1 Time-Dependent Failure Probability. In TRA, the LSF, expressed as $G(\mathbf{X}, \mathbf{Y}(t), t)$, represents the working state of an engineering system and contains the time parameter t. $\mathbf{X} = [X_1, X_2, \ldots, X_{n_X}]$ is a vector of random variables, $\mathbf{Y}(t) = [Y_1(t), Y_2(t), \ldots, Y_{n_Y}(t)]$ is a vector of stochastic processes as functions of t, and n_X and n_Y are the numbers of random variables and stochastic processes, respectively. In this article, a failure event occurs when the limit state function is less than zero at an arbitrary time within a specified time period $[0, T_L]$:

$$G(\mathbf{X}, \mathbf{Y}(t), t) < 0, \quad \exists t \in [0, T_L] \tag{1}$$

Hence, the time-dependent failure probability can be computed by

$$P_f(0, T_L) = \Pr\{G(\mathbf{X}, \mathbf{Y}(t), t) < 0), \quad \exists t \in [0, T_L]\} \tag{2}$$

Assuming $\mathbf{W} = [\mathbf{X}, \mathbf{Y}(t), t]$, Eq. (2) can be rewritten as follows:

$$P_f(0, T_L) = \int_0^{T_L} \int_{G(\mathbf{W})<0} f_W(w) dw dt \tag{3}$$

where $f_{\mathbf{W}}(w)$ is the joint probability density function of $\mathbf{W}$.

Although it is difficult to calculate the multiple integrals in Eq. (3) in practical engineering problems, the probability of failure can be calculated by MCS after constructing a response surrogate model $\hat{G}(\mathbf{X}, \mathbf{Y}(t), t)$ [19]:

$$P_f(0, T_L) = \frac{\sum_{j=1}^{N_{\text{MCS}}} I(\hat{G}(\mathbf{X}_j, \mathbf{Y}_j(t), t))}{N_{\text{MCS}}} \tag{4}$$

where N_{MCS} is the number of sample points and $I(\hat{G}(\mathbf{X}_j, \mathbf{Y}_j(t), t))$ is the time-dependent indicator function of $\hat{G}(\mathbf{X}, \mathbf{Y}(t), t)$:

$$I(\hat{G}(\mathbf{X}_j, \mathbf{Y}_j(t), t)) = \begin{cases} 1, & \text{if } \min\limits_{1 \le i \le s} (\hat{G}(\mathbf{X}_j, \mathbf{Y}_j(t_i), t_i) < 0 \\ 0, & \text{otherwise} \end{cases} \tag{5}$$

where s is the total number of discretized time nodes.

Notably, if a large number of DoE samples are needed to construct an accurate surrogate model, it is usually time consuming and not practical to construct a DT. Therefore, the efficient creation of an accurate surrogate model of LSF is one of the focuses of TRA in a DT. In this article, a kriging model is utilized as the surrogate model due to its wide investigation and applications. However, the STRA methodologies proposed in Sec. 3 may also be applicable for other surrogate types.

2.2 Kriging Model. A kriging model can predict not only the response but also the variance, which indicates the local uncertainty of the prediction [25]. Generally, a larger variance represents a larger uncertainty and lower robustness of the prediction. A kriging model consists of two parts, namely, a regression part and a stochastic process part, and is expressed as follows:

$$\hat{G}(\mathbf{x}) = \mathbf{f}^T(\mathbf{x})\boldsymbol{\beta} + Z(\mathbf{x}) \tag{6}$$

where $\mathbf{f}^T(\mathbf{x})$ is the basis regression function and $\boldsymbol{\beta}$ is the vector of regression coefficients. $\mathbf{f}^T(\mathbf{x})\boldsymbol{\beta}$ is the deterministic part, which represents the mean value of $\hat{G}(\mathbf{x})$. $Z(\mathbf{x})$ is a stationary Gaussian process with zero mean and a covariance. The covariance of two points $\mathbf{x}$ and $\mathbf{x}'$ is defined as follows:

$$\text{cov}(Z(\mathbf{x}), Z(\mathbf{x}')) = \sigma^2 R_\theta(\mathbf{x}, \mathbf{x}', \boldsymbol{\theta}) \tag{7}$$

where σ^2 is the process variance and $R_\theta(\mathbf{x}, \mathbf{x}', \boldsymbol{\theta})$ is the correlation function between the two points $\mathbf{x}$ and $\mathbf{x}'$ with the hyperparameter $\boldsymbol{\theta}$.

Among different correlation functions, the anisotropic squared-exponential correlation function (also called the anisotropic Gaussian model) is commonly selected in the field of reliability analysis [25]. It can be formulated as follows:

$$R_\theta(\mathbf{x}, \mathbf{x}', \boldsymbol{\theta}) = \prod_{k=1}^{d} \exp(-\theta_k (x_k - x_k')^2) \tag{8}$$

where d is the number of random variables $\mathbf{x}$, and x_k, x_k', and θ_k are the kth coordinates of $\mathbf{x}$, $\mathbf{x}'$, and $\boldsymbol{\theta}$, respectively. The kriging model with the anisotropic squared-exponential correlation function is utilized in this article.

2.3 Framework of Time-Dependent Reliability Analysis in a Digital Twin. For traditional TRA problems, once surrogate models are created based on training samples, they are often fixed and used to evaluate the reliability of an engineering system. However, the results may not be accurate because this approach does not consider the dynamic variation of the engineering system throughout its lifecycle. A single surrogate model probably cannot always accurately represent the relationship between the input variables and the evaluated performance. Thus, TRA in a DT inevitably requires continuously updating the surrogate model based on real-time measured data in a DT. A conceptual framework of TRA in a DT is shown in Fig. 1. The mature DT often has a six-dimensional architecture, including the physical system, digital model, sensor, service, actuator, and connection. The sensor supplies the real-time measured data for updating the digital state and the surrogate model for TRA. The predicted TRA results are used as real-time service data for the actuator to adjust or control the physical system. The connection provides the data transmission hardware and software and integrates the physical system and the digital model. Therefore, TRA in a DT needs to dynamically predict the time-dependent probability of failure of the physical system, which is one of key components of the DT service.

3 Proposed STRA Method

Although many TRA methods have been developed to reduce the computational burden and increase the analysis accuracy, the research on TRA for a DT still faces several challenges, as discussed in Sec. 1. This section elaborates a new STRA method to be utilized in a DT, particularly focusing on the stochastic process discretization and the adaptive sampling strategy.

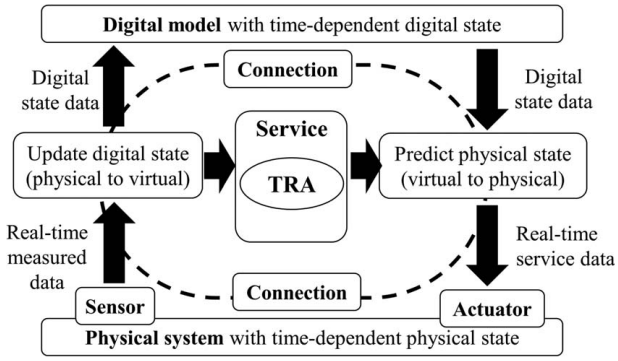

Fig. 1 Framework of TRA in a DT

3.1 Improved Expansion Optimal Linear Estimation. For TRA problems, EOLE [32] is often used to approximate the Gaussian stochastic process $Y(t)$ by a series of random variables $\mathbf{Z} = (Z_1, Z_2, \ldots, Z_p)$, which is expressed as follows:

$$Y(t) \approx \tilde{Y}(t) = \mu_Y(t) + \sigma_Y(t) \sum_{i=1}^{p} \frac{1}{\sqrt{\lambda_i}} \mathbf{\Phi}_i Z_i \boldsymbol{\rho}_Y(t) \tag{9}$$

where p is the number of dominant eigenvalues, which should be smaller than or equal to the number of discrete time nodes s; $\mu_Y(t)$ is the mean function; $\sigma_Y(t)$ is the standard deviation function of $Y(t)$; Z_i is the independent standard normal variable; $\boldsymbol{\rho}_Y(t) = [\rho_Y(t, t_1), \rho_Y(t, t_2), \ldots, \rho_Y(t, t_i), \ldots, \rho_Y(t, t_s)]^T$ is a vector of the correlation function; $t_i (i = 1, 2, \ldots, s)$ are the discrete time nodes; and λ_i and $\mathbf{\Phi}_i$ are the eigenvalues and eigenvectors, respectively, of the correlation matrix C_Y. The correlation matrix C_Y is expressed as follows:

$$\mathbf{C}_Y = \begin{bmatrix} \rho_Y(t_1, t_1) & \rho_Y(t_1, t_2) & \cdots & \rho_Y(t_1, t_s) \\ \rho_Y(t_2, t_1) & \rho_Y(t_2, t_2) & \cdots & \rho_Y(t_2, t_s) \\ \vdots & \vdots & \ddots & \vdots \\ \rho_Y(t_s, t_1) & \rho_Y(t_s, t_2) & \cdots & \rho_Y(t_s, t_s) \end{bmatrix}_{s \times s} \tag{10}$$

where $\rho_Y(t_i, t_j)$ is the autocorrelation coefficient function.

The improved EOLE proposed in this article determines two parameters: the number of discrete time nodes s and the number of dominant eigenvalues p. First, we explain the determination of p given s. For a given s, the calculated eigenvalues of the correlation matrix are first ranked in a descending order, and the largest p eigenvalues are selected as the dominant eigenvalues. p is selected to satisfy the following inequality:

$$\frac{\sum_{i=1}^{p} \lambda_i}{\sum_{i=1}^{s} \lambda_i} > \eta \tag{11}$$

where the threshold η is set to 0.99 in this article. Therefore, the stochastic process $Y(t)$ can be represented by p independent standard normal variables $\mathbf{Z} = (Z_1, Z_2, \ldots, Z_p)$.

The determination of s is explained as follows. Obviously, different s values will result in different correlation matrices and different stochastic process discretization accuracies. In addition, the s value will affect the calculation time of the TRA and, consequently, the real-time RA requirement of a DT. The current EOLE method usually adopts a conservative solution, i.e., using a large s value to avoid inaccurate discretization, which will inevitably increase the computational time of the TRA. The STRA method proposed in this article uses the variance of the stochastic process discretization error to select the best number of discrete time nodes s. The variance of the prediction error at the jth test time node t_j is given by Eq. (12), whose detailed derivation process can be found in Ref. [32].

$$\mathrm{Var}[Y(t_j) - \tilde{Y}(t_j)] = \sigma_Y^2(t_j) - \sum_{i=1}^{p} \frac{1}{\lambda_i} (\mathbf{\Phi}_i^T \rho_Y(t_j))^2 \tag{12}$$

For each discretized stochastic process given s, the average error variance over a large number of test time nodes is set as the discretization error of the stochastic process, which is expressed as follows:

$$m\mathrm{Var} = \frac{\sum_{j=1}^{S} \mathrm{Var}[Y(t_j) - \tilde{Y}(t_j)]}{S} \tag{13}$$

where S is the number of test time nodes uniformly distributed in $[0, T_L]$. Here, $S = 10^6$. The test time nodes $t_j (j = 1, 2, \ldots, S)$ are used to calculate the average error variance in Eq. (13), which are different from the discrete time nodes $t_i (i = 1, 2, \ldots, s)$ for approximating the Gaussian stochastic process in Eq. (9).

If there are several stochastic processes in a TRA problem, the discretization error of all the stochastic processes is equal to the sum of the average variances of the errors of all the stochastic processes. Among all the candidate s values, the value corresponding to the minimum discretization error is selected for discretizing the stochastic process(es). Compared with the traditional EOLE strategy, this new stochastic process discretization strategy avoids selecting an overly large value of s, which would impose an unnecessary computational burden, while guaranteeing the discretization accuracy. The dynamic selection of suitable s and p values for different stochastic processes is demonstrated in the case studies in Sec. 4.

In addition to the aforementioned endeavor in stochastic process discretization, we have investigated different types of inputs of the kriging model. For the LSF with multiple stochastic processes $\mathbf{Y}(t)$, traditionally, the input of the kriging model for $G = g(\mathbf{X}, \mathbf{Y}(t), t)$ is $[X, (Z_1, \ldots, Z_{n_Y}), t]$ based on EOLE [19]. Therefore, the dimension of the input of the kriging model is equal to $n_X + \sum_{i=1}^{n_Y} p_i + 1$. This input dimension will be huge if the number of stochastic processes in $\mathbf{Y}(t)$ is large. In this article, after the stochastic process discretization, the approximated stochastic processes $\tilde{\mathbf{Y}}(t)$ are directly used to construct the surrogate model rather than using the discretized random variables $\mathbf{Z} = (Z_1, Z_2, \ldots, Z_p)$ as part of the input of the surrogate model. As a result, the input dimension of the kriging model for $G = g(\mathbf{X}, \mathbf{Y}(t), t)$ is only $n_X + n_Y + 1$, which is significantly decreased, speeding up the calculation of the TRA.

3.2 Sensitive Voronoi Cells. The proposed STRA method aims to improve the efficiency of constructing the kriging model by sampling in the regions with large failure probability prediction errors and shifts the adaptive sampling domain from the global space to the vicinity of the LSF. Two major issues need to be addressed: (1) properly partitioning the sampling space and (2) identifying the sensitive regions near the LSF.

3.2.1 Partitioning the Sampling Region Based on Voronoi Tessellation. Voronoi tessellation [34] is used to divide the entire design space into regions/cells close to each of a given set of existing samples $A = \{a_1, a_2, \ldots, a_m\} \in \mathbb{R}^d$, and m is the number of existing samples. According to the sample set A, the entire design space is divided into a set of Voronoi cells $C = \{C_1, C_2, \ldots, C_m\}$, each of which is defined by [35]

$$C_i = \bigcap_{a_j \in A \setminus a_i} \mathrm{dom}(a_i, a_j) \tag{14}$$

where $A \setminus a_i$ is the existing sample set excluding the sample a_i and $\mathrm{dom}(a_i, a_j)$ includes all points close to a_i in a half plane bounded by the perpendicular bisector of a_i and a_j, which is defined as follows:

$$\mathrm{dom}(a_i, a_j) = \{a \in \mathbb{R}^d | \| a - a_i \|_2 \leq \| a - a_j \|_2\} \tag{15}$$

The candidate samples in the entire design space are first generated by the MCS method, as demonstrated by the dots in the two-dimensional example in Fig. 2. The triangles in Fig. 2 are the existing samples. All the candidate samples are then categorized into each Voronoi cell based on the Voronoi tessellation.

3.2.2 Identification of Sensitive Voronoi Cells. For efficient TRA, each new sample is expected to contribute to the improvement of the accuracy of reliability analysis using the surrogate model. To select samples more efficiently, it is necessary to filter out the Voronoi cells with large prediction errors. Traditionally, LOO cross-validation [36] is often used to calculate the prediction error and identify sensitive Voronoi cells. The prediction error e_{LOO}^i based on traditional LOO cross-validation is calculated as follows:

$$e_{\mathrm{LOO}}^i = |g(a_i) - \hat{g}_{A \setminus a_i}(a_i)| \tag{16}$$

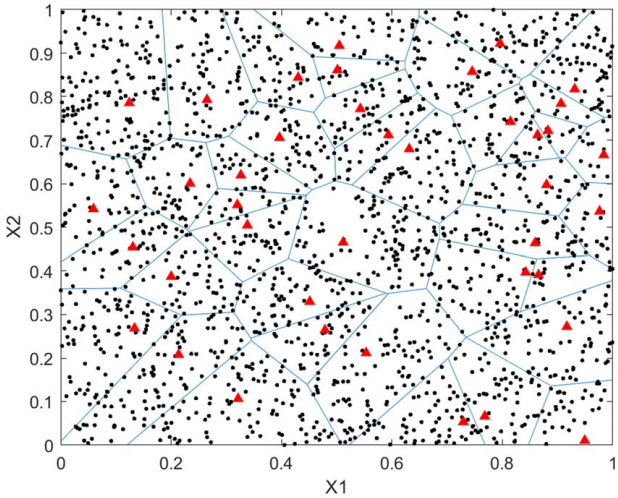

Fig. 2 Example of two-dimensional Voronoi tessellation

where $g(a_i)$ denotes the real response at a_i and $\hat{g}_{A\setminus a_i}(a_i)$ is the response at a_i predicted by the kriging model based on the sample set $A \setminus a_i$.

Traditionally, the Voronoi cell with the largest predicted response error is selected as the sensitive Voronoi cell [33]. However, this may result in the selection of a Voronoi cell with a large error that is not in the vicinity of the limit state function, which may not influence the accuracy of the reliability analysis very much. In this article, a modified LOO cross-validation method is developed using the error of the failure probability to guide the selection of sensitive Voronoi cells. The modified LOO cross-validation error $e^i_{\text{LOO}*}$ at a point a_i is defined as follows:

$$e^i_{\text{LOO}*} = |\hat{P}_f - \hat{P}_f^{A\setminus a_i}| \tag{17}$$

where $\hat{P}_f$ is the predicted failure probability evaluated by using the sample set A and $\hat{P}_f^{A\setminus a_i}$ is the predicted failure probability evaluated by using the sample set $A \setminus a_i$. The aforementioned process is repeated for each point in A, and the failure probability errors for all existing samples are obtained.

It is observed that a large failure probability error $e^i_{\text{LOO}*}$ indicates that inserting new sample(s) into the cell C_i in which a_i is located will probably improve the accuracy of the probability failure calculation by the surrogate model. To identify the sensitive cells, the average failure probability error $\bar{e}_{\text{LOO}*}$ is first calculated as follows:

$$\bar{e}_{\text{LOO}*} = \frac{\sum_{i=1}^{m} e^i_{\text{LOO}*}}{m} \tag{18}$$

where m is the number of Voronoi cells. Traditionally, the Voronoi cell with the largest e^i_{LOO} or $e^i_{\text{LOO}*}$ value is identified as the most sensitive cell, into which a new training sample is inserted for surrogate modeling in each iteration (e.g., Ref. [28]). Here, multiple sensitive Voronoi cells, denoted $C^i_{\text{sensitive}}$, $i = 1, 2, \ldots, q$, are identified as the cells whose failure probability error $e^i_{\text{LOO}*}$ is larger than the average failure probability error $\bar{e}_{\text{LOO}*}$. Notably, (1) the identified sensitive cells are expected to be in the vicinity of the LSF and (2) the Voronoi cells will be repartitioned in each sampling iteration after a new sample is selected from candidate samples in the identified sensitive cells. The rationale for selecting this new sample for updating the surrogate model is explained in Sec. 3.3.

3.3 Weighted Expected Feasibility Function. After the sensitive Voronoi cells are selected, the next step is to select new training samples among all the candidate MCS samples in the sensitive cells to update the kriging model. A common method for selecting new training samples is to use an active learning strategy with a learning function, which helps improve the efficiency of constructing the kriging model. One of the most popular learning functions used to identify new training samples of the adaptive kriging model is the expected feasibility function (EFF) proposed in the efficient global reliability analysis algorithm [37]. The EFF tends to select points that are close to the LSF with high uncertainty [37]. It is expressed as follows:

$$\begin{aligned}\text{EFF}(x) = {} & \mu_{\hat{G}}(x)\left[2\Phi\left(\frac{-\mu_{\hat{G}}(x)}{\sigma_{\hat{G}}(x)}\right) - \Phi\left(\frac{-\varepsilon(x) - \mu_{\hat{G}}(x)}{\sigma_{\hat{G}}(x)}\right) - \Phi\left(\frac{\varepsilon(x) - \mu_{\hat{G}}(x)}{\sigma_{\hat{G}}(x)}\right)\right] \\ & - \sigma_{\hat{G}}(x)\left[2\phi\left(\frac{\mu_{\hat{G}}(x)}{\sigma_G(x)}\right) - \phi\left(\frac{-\varepsilon(x) - \mu_{\hat{G}}(x)}{\sigma_G(x)}\right) - \phi\left(\frac{\varepsilon(x) - \mu_{\hat{G}}(x)}{\sigma_G(x)}\right)\right] \\ & + \varepsilon(x)\left[\Phi\left(\frac{\varepsilon(x) - \mu_{\hat{G}}(x)}{\sigma_{\hat{G}}(x)}\right) - \Phi\left(\frac{-\varepsilon(x) - \mu_{\hat{G}}(x)}{\sigma_{\hat{G}}(x)}\right)\right]\end{aligned} \tag{19}$$

where ϕ is the standard normal probability density function; Φ is the standard normal cumulative distribution function; $\varepsilon(x)$ is the tolerance, which is set to $2\sigma_{\hat{G}}(x)$; and $\mu_{\hat{G}}(x)$ and $\sigma_{\hat{G}}(x)$ are the predicted mean and standard deviation, respectively, for sample x.

Traditionally, the candidate sample corresponding to the largest EFF value in a sensitive cell is selected as the new training sample. However, it has been reported that the EFF sometimes generates useless samples when the kriging model is accurate enough in some local areas [28]. To consider the importance of the modified LOO cross-validation error of the failure probability (Eq. (18)), a WEFF is proposed to further enhance the sampling efficiency of the EFF and decrease the number of training samples. For each sensitive Voronoi cell $C^i_{\text{sensitive}}$, $i = 1, 2, \ldots, q$, there is a corresponding weight, which is expressed as follows:

$$\text{weight}(i) = \frac{e^i_{\text{LOO}*}}{\max\left(e_{\text{LOO}*}\right)} \tag{20}$$

where $\max(e_{\text{LOO}*})$ is the maximum failure probability error over all the identified sensitive cells.

The WEFF value of a candidate point x in the sensitive Voronoi cell $C^i_{\text{sensitive}}$ is defined as follows:

$$\text{WEFF}(x) = \text{weight}(i) \times \text{EFF}(x) \tag{21}$$

Among all the candidate samples in the sensitive Voronoi cells, the sample corresponding to the largest WEFF value is selected as the new training sample to be added to update the surrogate model. In this way, the kriging model is iteratively updated until the following stopping criterion is satisfied:

$$\varepsilon_{\max} \le \varepsilon_{\text{tar}} \tag{22}$$

where $\varepsilon_{\max}$ is the predicted error, which can be calculated according to the maximum real-time estimation error calculation method [30], and ε_{tar} is the target prediction error, which is equal to 0.05 in this

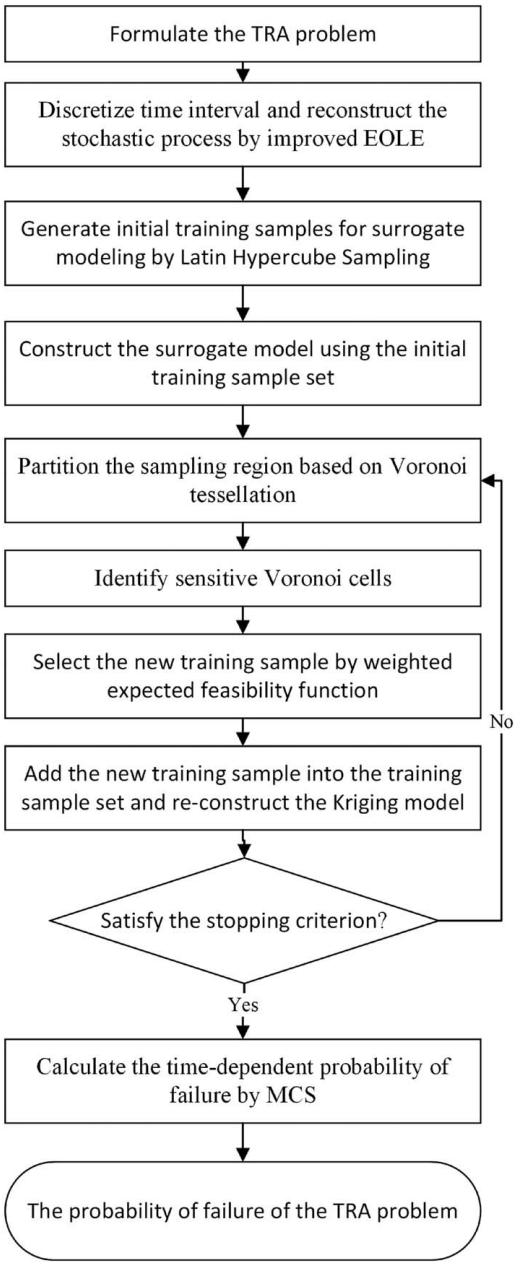

Fig. 3 Flowchart of the proposed STRA method

article [30]. After the surrogate models $\hat{G}(\mathbf{X}, \mathbf{Y}(t), t)$ are successfully constructed, the time-dependent probability of failure can be instantly calculated by MCS through Eq. (4). A flowchart of the proposed STRA method is shown in Fig. 3.

4 Case Studies, Results, and Discussion

In this section, the proposed STRA method is tested on a mathematical example, a corroded beam structure case, and a realistic engineering problem used for a DT application. The performance of the proposed STRA method is thoroughly investigated and compared with those of three state-of-the-art TRA methods, namely, *t*-IRS [21], eSPT [38], and REAL [30]. The TRA results estimated by MCS are used as a benchmark. To account for the statistical uncertainty associated with random sampling, for the mathematical example and the corroded beam structure case, we repeat the experiments using all these methods five times independently for a more credible comparison. All the case studies are conducted using a computer (Inter(R) Core(TM) i7-10700H CPU@2.90 GHz processor with 64 GB RAM and a 64-bit Windows operating system).

Table 1 Statistical parameters of the random variables and the stochastic process used in the first case study

Random variable or stochastic process	Distribution type	Mean	Standard deviation	Autocorrelation function
X_1	Normal	3.5	0.25	–
X_2	Normal	3.5	0.25	–
$Y(t)$	Gaussian process	0	1	$\exp(-(t_2-t_1)^2)$

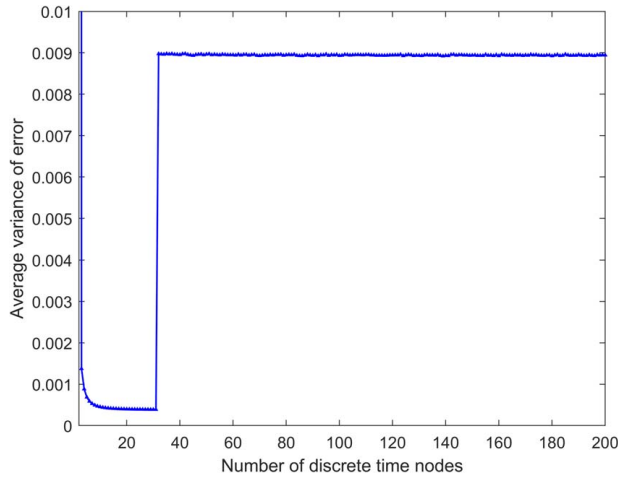

Fig. 4 Relation between the average variance of the error and the number of discrete time nodes in the first case study

4.1 Time-Dependent Reliability Analysis of a Numerical Model. The first case study is the TRA of a numerical model from Ref. [19]. Its performance function is defined by

$$G(\mathbf{X}, \mathbf{Y}(t), t) = -20 + X_1^2 X_2 - 5X_1(1 + Y(t))t + (X_2 + 1)t^2 \quad (23)$$

where t represents the time parameter, which varies from 0 to 1; $\mathbf{X} = [X_1, X_2]$ denotes two independent random variables; and $\mathbf{Y}(t)$ is a Gaussian process. The statistical parameters of the random variables and the stochastic process are shown in Table 1.

Both the number of discrete time nodes s and the number of dominant eigenvalues p need to be predefined for the discretization of a stochastic process. The relationship between the average variance of the error and the number of discrete time nodes, as shown in Fig. 4, is first investigated using the improved EOLE method. The average variance of the error based on Eq. (13) decreases monotonically as the number of discrete time nodes increases from 0 to 31, while it increases dramatically when $s = 32$. The reason is that when $s = 31$, p based on Eq. (11) equals 3, while $p = 2$ if $s = 32$ based on Eq. (11), which results in a huge jump in the average variance of the error from $s = 31$ to $s = 32$ in this case. Therefore, it is vital to properly determine the number of discrete time nodes and the number of dominant eigenvalues to approximate the stochastic processes for different TRA problems. For a fair comparison, the number of discrete time nodes s is set to 31 in this case.

Similar to Ref. [19], 12 initial samples are first generated by the Latin hypercube sampling method [39], and the time-dependent probability of failure is calculated using the proposed STRA method. Figure 5 illustrates the failure probability over the normalized time interval. All the tested methods obtain convincing results at early time moments (e.g., $t \le 0.7$); however, at late time moments

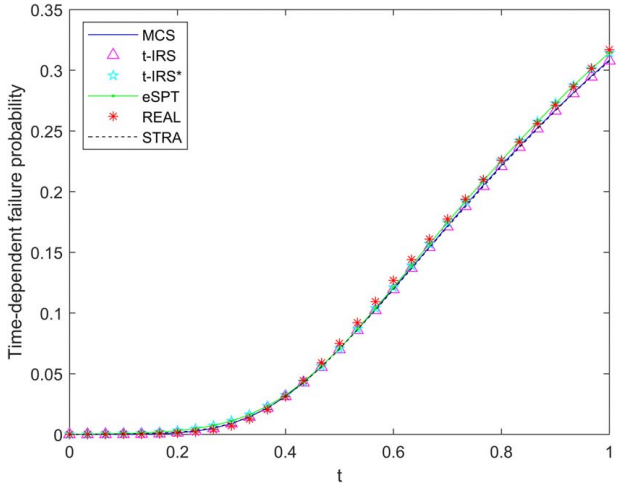

Fig. 5 Time-dependent failure probability calculated by different methods in the first case study

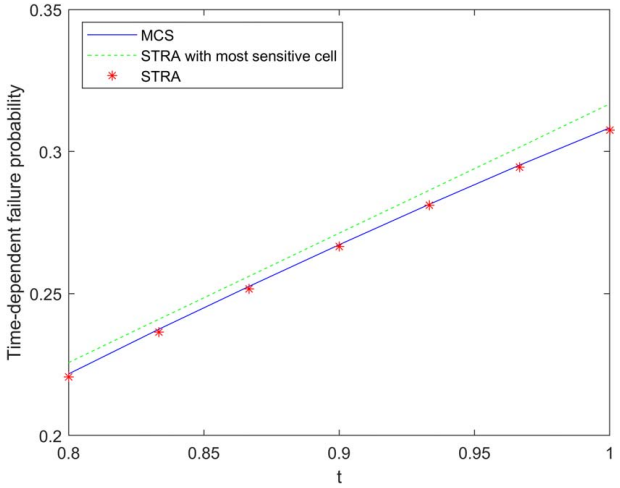

Fig. 6 Comparison of the time-dependent failure probabilities calculated by STRA with the most sensitive cell and with multiple sensitive cells in the first case study

Table 2 Reliability analysis results of the first case study

Method	NFE	P_f	Error (%)	T_1 (s)	T_2 (s)
MCS	10^6	0.307814	–	–	–
t-IRS	80.3	0.308050	0.08	22.7	29.2
t-IRS*	35.4	0.313080	1.71	791.4	31.6
eSPT	48.1	0.299643	2.65	73.2	29.8
REAL	32.1	0.299636	2.66	636.7	31.9
STRA	27.4	0.304104	1.20	1675.8	29.9

(e.g., $t>0.7$), the proposed STRA method and the t-IRS method produce more accurate time-dependent failure probabilities than the REAL method and the eSPT method. As shown in Table 2, although the error of the failure probability calculated by the proposed STRA method (1.20%) is larger than that calculated by the t-IRS method (0.08%), the proposed STRA method requires the smallest number of function evaluations (NFEs) among the four tested methods. This indicates that the proposed STRA method can efficiently create a surrogate model using fewer DoE samples, which is important for the application in a DT. In order to further compare the efficiency, the convergence criterion of the original t-IRS method in Ref. [21] is replaced by the same convergence criterion used in the proposed STRA method in this article, and is denoted by t-IRS*. It can be seen from Table 2 that under the same convergence criterion, the efficiency and accuracy of t-IRS* are not as good as those of STRA. In addition, in Table 2, T_1 represents the time to construct the surrogate models, and T_2 represents the time of reliability analysis using the surrogate models. In this numerical case, the STRA method requires the largest model training time due to the complexity of this method, while the reliability analysis times of the five tested methods are similar after the surrogate models are constructed. The results in Table 2 are the averages of the results from five TRA tests.

In addition, the number of discrete time nodes in the five methods in Table 2 is all equal to 31 (i.e., $s=31$), whereas the number of discrete time nodes in the REAL method in the Ref. [30] is 101. The calculation time of the time-dependent failure probability T_2 of the proposed STRA method, when using 31 and 101 discrete time nodes, is equal to 29.9 s and 167.5 s, respectively, using the same computer. This indicates that by dynamically considering the number of discrete time nodes of the stochastic process, the proposed STRA method can achieve not only accurate TRA results but also a short computation time for the TRA process, which is essentially important for a DT. Fast surrogate modeling and quick reliability evaluation are essential for the real-time performance of DTs.

Moreover, the effect of using multiple sensitive cells in each sampling iteration is studied. As shown in Fig. 6, the time-dependent failure probability calculated based on the proposed STRA method using multiple sensitive cells is consistently more accurate than that calculated based on the STRA method using the most sensitive cell as the sampling region in each iteration. It is possible that the method considering only the most sensitive cell may prematurely terminate the sampling process when constructing the surrogate model.

4.2 Time-Dependent Reliability Analysis of a Corroded Beam Structure. The second case study is the TRA of a corroded beam structure from Ref. [40], as shown in Fig. 7. The length of the beam, L, is 5 m, and the cross section is rectangular with an initial width b_0 and height h_0. Considering that the beam is affected by gravity, a uniformly distributed load $p=\rho_{st}b_0h_0$ N/m is used, where $\rho_{st}=78.5$ kN/m^3 is the steel density. In addition, the beam is subjected to a concentrated force $F(t)$ at the center point.

The beam will be corroded by external effects such as raindrop erosion during its lifecycle. Its cross-sectional area is assumed to linearly decrease with time, and the mechanical strength of the corroded area will be gradually lost. The remaining uncorroded cross-

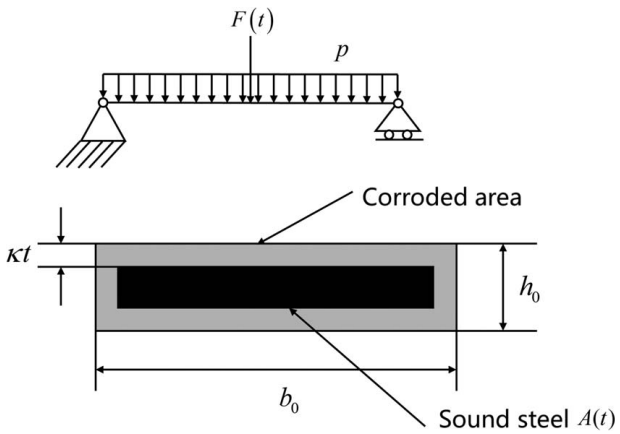

Fig. 7 Second case study: TRA of a corroded beam structure

Table 3 Statistical information on the random parameters of the corroded beam structure

Parameter	Distribution	Mean	Standard deviation	Autocorrelation function
f_y	Lognormal	240 MPa	24 MPa	–
b_0	Lognormal	0.2 m	0.01 m	–
h_0	Lognormal	0.03 m	0.003 m	–
$F(t)$	Gaussian process	3500 N	700 N	$\exp(-(t_2-t_1)^2/\lambda^2)$

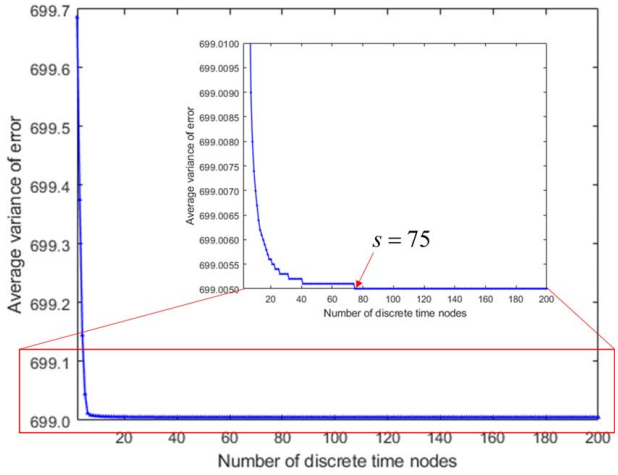

Fig. 8 Relation between the average variance of the error and the number of discrete time nodes in the second case study

sectional area $A(t)$ can be expressed as follows:

$$A(t) = b(t) \times h(t) \tag{24}$$

where $b(t) = b_0 - 2\kappa t$, $h(t) = h_0 - 2\kappa t$, and $\kappa = 0.03$ mm/year denote a constant corrosion rate, and t represents the time parameter, which varies within [0, 20] years.

The performance function of the corroded beam can be expressed as follows:

$$G(\mathbf{X}, \mathbf{Y}(t), t) = M_u(t) - M(t) = \frac{b(t)h^2 f_y}{4} - \left(\frac{F(t)L}{4} + \frac{\rho_{st} b_0 h_0 L^2}{8}\right) \tag{25}$$

where $M_u(t) = b(t)h^2(t)f_y/4$ is the ultimate bending moment capacity of the beam and f_y is the steel yield stress. The bending moment at the midpoint of the beam is the largest, which can be expressed as follows:

$$M(t) = ((F(t)L/4) + (\rho_{st} b_0 h_0 L^2/8)) \tag{26}$$

We let $\mathbf{X} = [f_y, b_0, h_0]$ be lognormally distributed random variables, $F(t)$ be a Gaussian process, and the correlation parameter λ in the autocorrelation function be equal to 5 years by referring to Ref. [21]. Detailed statistical information on the random variables and the stochastic process is presented in Table 3.

According to Eq. (13), the relationship between the average variance of the error and the number of discrete time nodes is illustrated in Fig. 8. As shown in Fig. 8, the average variance of the error significantly decreases as s increases. Once s reaches 75, the average variance of the error does not decrease further. Therefore, the number of discrete time nodes s is set to 75 in this case. To reconstruct the stochastic process $F(t)$, it is necessary to use six standard normal distribution random variables $\mathbf{Z} = [Z_1, Z_2, \ldots, Z_6]$ based on Eq. (11) (i.e., $p = 6$). Additionally, the number of initial samples for surrogate modeling is set to 40 in this case.

The results of different methods are compared in Table 4, which are averages of the results from five TRA tests. It is observed from the table that the four methods have high accuracy in evaluating the time-dependent failure probability (with a failure probability of less than 5%), which can also be observed from Fig. 9. t-IRS has the minimum error among them; however, it has a large computational burden (i.e., the largest NFE among the four methods). In addition, the t-IRS* method is not as efficient and accurate as STRA, as shown in Table 4. The proposed STRA requires the smallest NFE of 56.4 on average, which reduces the computational cost of surrogate modeling by 67.1%, 50.3%, and 6.93% compared to t-IRS, eSPT, and REAL, respectively. Although both REAL and STRA yield better tradeoffs between accuracy and efficiency than t-IRS and eSPT, the smaller NFE and the higher TRA accuracy demonstrate the superiority of the proposed STRA method. In this corroded beam case, the STRA method requires the largest T_1.

Table 4 Reliability analysis results of the second case study

Method	NFE	P_f	Error (%)	T_1 (s)	T_2 (s)
MCS	10^6	0.04719	–	–	–
t-IRS	171.4	0.04714	0.11	48.4	157.9
t-IRS*	74.1	0.04780	1.29	8003.4	158.0
eSPT	113.4	0.04880	3.41	370.9	161.5
REAL	60.6	0.04816	2.06	4136.0	159.4
STRA	56.4	0.04776	1.21	12381.6	158.1

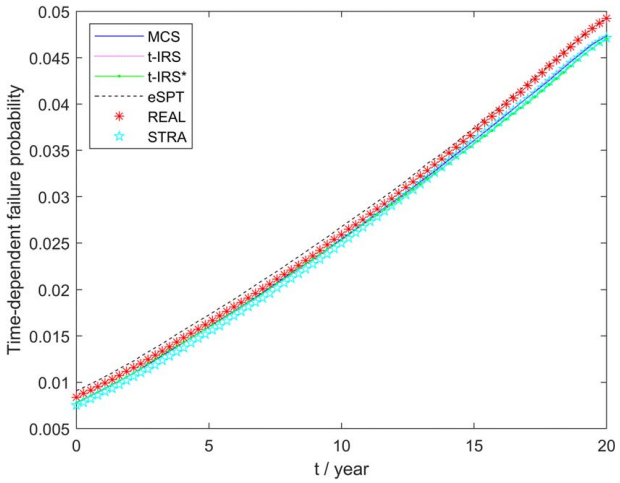

Fig. 9 Time-dependent failure probability calculated by different methods in the second case study

4.3 Time-Dependent Reliability Analysis of a Cutterhead in a Digital Twin of a Tunnel Boring Machine. Tunnel boring machines (TBMs) have been widely used for tunnel excavation because of their high efficiency, safety, and environmental friendliness compared to conventional blasting excavation. The cutterhead, located at the front of a TBM, suffers from fatigue damage due to the complex interaction between it and the soil during TBM operation. To ensure the proper design and safe operation of a TBM, it is

Fig. 10 A DT of a TBM and the TRA of the cutterhead of the TBM

Table 5 Parameters and corresponding values used in the TRA of the cutterhead of a TBM

Parameter	Value
Diameter of the cutterhead D	6.65 m
Opening ratio of the cutterhead ξ	0.33
Pressure value on the chest plate p_c	1.8 bar
Length of the soil tank l	2 m
Coefficient of friction between soil and steel f_1	0.25
Buried depth of the shield axis H	18 m
Length of the main shield machine L	9.01 m
Total weight of the TBM W	450×10^3 kg
Width of the cutterhead B	0.3 m
Friction angle φ	19.3 deg
Cohesion of the soil c	19.8 N
Advancing speed of the cutterhead v	50 mm/min
Speed of the cutterhead ω	1 rpm
Depth of soil covering of the mixing blade H_0	21.34 m
Diameter of the mixing blade D_b	0.1 m
Length of the mixing blade L_b	0.6 m
Distance from the mixing blade to the center of the cutterhead R_b	1.84 m
Soil coefficient of friction with steel f_2	0.09
Number of stirring rods m	2
Number of blocks of the cutterhead k	6
Yield strength of the cutterhead δ_S	225 MPa

essential to accurately predict the time-dependent reliability of the cutterhead. A DT of a TBM has been constructed and used to monitor the operating status and to guide operation and maintenance. The construction of the DT of the TBM is beyond the scope of this article and will be explained in detail in our future work. The proposed STRA method is applied to conduct the TRA of the cutterhead considering the complex loading uncertainty during the tunnel boring process, as shown in Fig. 10.

The geological loading calculation method proposed by Chen et al. [41] is used to calculate the thrust F and the torque T of the cutterhead of the TBM in a complex geological environment.

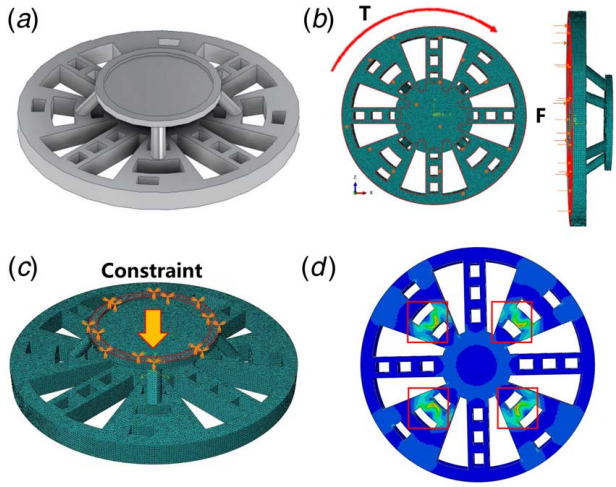

Fig. 11 FEA modeling process of the cutterhead of a TBM

The thrust F and the torque T are formulated as follows:

$$F=\frac{\pi D^2}{4}(p_0+\Delta p_2)(1-\xi)+\frac{\pi D^2}{4}p_c e^{Al}\xi + f_1\gamma' D\left[2(1+K_a)H-\frac{1}{4}D(\pi+2K_a)\right]L+f_1 W \tag{27}$$

$$T=\frac{\pi D^3}{12}f_1(K_0\gamma' H+\Delta p_2)(1-\xi)+\frac{\pi D^2}{4}f_1\gamma' HB(1+K_0) + \left[p_0\tan^2\left(\frac{\pi}{4}+\frac{\varphi}{2}\right)+2c\tan\left(\frac{\pi}{4}+\frac{\varphi}{2}\right)\right]\frac{D^2}{8}\frac{v}{\omega}+\gamma' H_0 D_b L_b R_b f_2 m \tag{28}$$

$$p_0=K_0 H(\gamma'+10) \tag{29}$$

Table 6 Statistical information on the random parameters used in the TRA of the cutterhead of a TBM

Parameter	Distribution	Mean	Standard deviation	Autocorrelation function
K_a	Normal	0.3933	0.019665	–
K_0	Normal	0.6694	0.03347	–
$\mu(t)$	Gaussian process	0.28	0.014	$\exp(-(t_2-t_1)^2/5^2)$
$E_u(t)$	Gaussian process	63 MPa	3.15 MPa	$\exp(-(t_2-t_1)^2/5^2)$
$\gamma'(t)$	Gaussian process	8.718 KN/m^3	0.4359 KN/m^3	$\exp(-(t_2-t_1)^2/4^2)$

$$\Delta p_2 = \frac{10.13(1-\mu)E_u}{(1+\mu)(3-4\mu)D}\frac{\pi v(1-\xi)^2}{k\omega} \tag{30}$$

$$A = \frac{4\tan\varphi}{D}\frac{1-\mu}{\mu} \tag{31}$$

where γ' is the effective gravity of the soil, K_a is the coefficient of active earth pressure, K_0 is the coefficient of static earth pressure, E_u represents the Young's modulus of the soil, μ is the Poisson's ratio of the soil, and other parameters are shown in Table 5.

In this case study, the TRA of a TBM cutterhead with a diameter of 6.28 m (Fig. 11(*a*)) is investigated. ABAQUS is used for mesh generation and stress calculation by finite element analysis (FEA). The FEA model of the cutterhead has 584,252 elements and 120,706 nodes. The thrust F and the torque T are applied at a node rigidly coupled with the cutterhead at the center of the cutter hole (Fig. 11(*b*)). The back of the cutterhead is fixed as a constraint (Fig. 11(*c*)). As a representation of the stress results, a von Mises stress contour under $F = 1.8728 \times 10^7$ N and $T = 1.2719 \times 10^9$ Nm is shown in Fig. 11(*d*). Hot areas with large stresses are distributed at the four junctions of the cutterhead, where fatigue cracks are often observed in the real cutterhead.

On the basis of collected data from geological measurements by the collaborating TBM manufacturing company, we reasonably assume that during the tunneling process, the active earth pressure coefficient K_a and the static earth pressure coefficient K_0 follow normal distributions and that Poisson's ratio of the soil μ, Young's modulus of the soil E_u, and the effective weight of the soil γ' follow Gaussian processes. t denotes the time parameter, which varies within [0, 20] years. Statistical information on these random parameters is listed in Table 6. To evaluate the failure of the cutterhead, the average of the top 100 stress values in the four hot areas $\bar{\sigma}(t)$ is compared with the allowable strength δ_S. If $\bar{\sigma}(t)$ is greater than δ_S, a failure is identified. Therefore, the performance function of the cutterhead can be expressed as follows:

$$G(K_a, K_0, \mu(t), E_u(t), t) = \delta_S - \bar{\sigma}(t) \tag{32}$$

The number of discrete time nodes s is calculated based on the improved EOLE method. As shown in Fig. 12, s is selected to be 116, as the average variance of the error does not decrease when $s > 116$. The number of initial training samples is set to 12. The total size of the candidate sample pool is 5×10^5. It is not affordable to apply the MCS method in this engineering problem due to the extremely large computational time. It is also found that the t-IRS method and the eSPT method are computationally very expensive (they require more than 300 samples to finish the TRA); thus, they are obviously not appropriate for use for a DT. Although the REAL method and the proposed STRA method obtain similar failure probabilities (see Fig. 13; the P_f values calculated by REAL and STRA are 0.0076 and 0.0074, respectively), the proposed STRA method has a much higher efficiency (NFE = 105) than the REAL method (NFE = 173).

The computational time of surrogate model training (T_1) and the reliability analysis time (T_2) using the trained surrogate model based on the STRA method are compared with the counterparts based on the REAL method. In this engineering case, T_1 of the STRA method and the REAL method is 27.4 h and 41.8 h, respectively, while T_2 of the STRA method and the REAL method is 1513.9 s and 1518.8 s, respectively. By reducing the training points, the STRA method can greatly improve the efficiency of surrogate model training. Hence, the proposed STRA method can accurately and efficiently handle the TRA of the TBM cutterhead and is the most suitable for a DT.

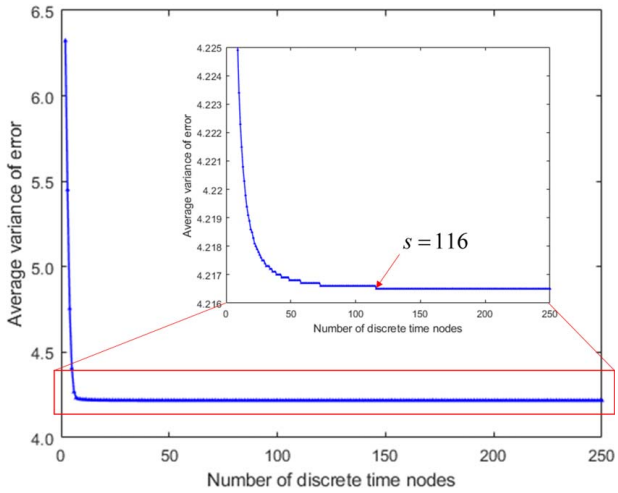

Fig. 12 Relation between the average variance and number of discrete time nodes in the third case study

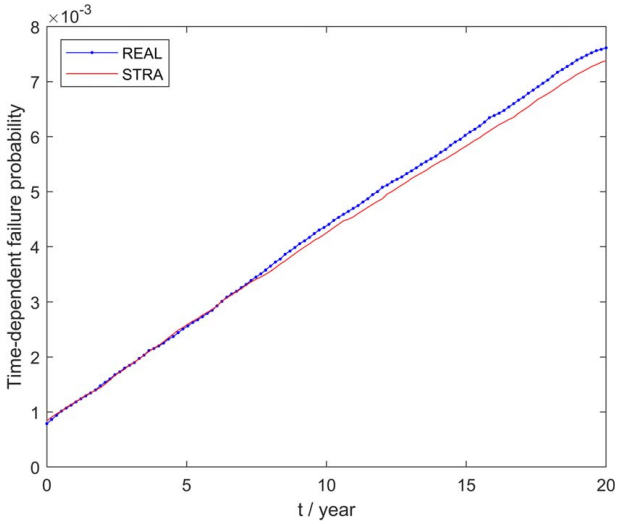

Fig. 13 Time-dependent failure probability of the cutterhead of the TBM

5 Conclusions

This article presents a highly efficient surrogate-based time-dependent reliability analysis method for a digital twin. This method discretizes stochastic processes through improved EOLE and identifies sensitive Voronoi cells to convert the sampling domain from the whole design space to the vicinity of the limit

state boundary. A weighted learning function is proposed for iteratively selecting new sample points from the identified sensitive Voronoi cells. The proposed method constructs a kriging model with high efficiency and calculates the real-time time-dependent failure probability through MCS.

The comparison results of the TRA of a numerical model, a corroded beam structure, and a cutterhead of a TBM demonstrate the superiority of the proposed STRA method for a DT over existing methods, specifically in the following aspects: (1) the proposed STRA method dynamically selects as few discrete time nodes as possible for the stochastic processes while maintaining the discretization accuracy; (2) by using multiple sensitive Voronoi cells and a weighted expected feasibility function, it effectively reduces the number of DoE sample points, which enables the DT to quickly construct an accurate time-dependent surrogate model; and (3) the DT utilizes the time-dependent surrogate model constructed based on the proposed STRA method to accurately and efficiently carry out the TRA process. Based on the results of the three case studies, the proposed STRA method is the most suitable method for a DT due to its good balance between accuracy and efficiency for TRA.

Correlations between variables are inevitable in both the physical and digital worlds. In the future work, the proposed method will be extended to TRA considering the correlations between variables. In addition, time-dependent reliability-based design optimization utilizing the methodologies proposed in this article merits investigation.

Acknowledgment

The authors gratefully acknowledge the support from the National Natural Science Foundation of China (NSFC), the Zhejiang Provincial Natural Science Foundation of China, the State Key Laboratory of Fluid Power and Mechatronic Systems, and the international cooperation program managed by the National Research Foundation of Korea. The authors also thank the reviewers and the editors for their insightful comments, which helped improve the quality of the paper.

Funding Data

- National Natural Science Foundation of China (NSFC) (Grant Nos. 52275275 and 52111540267; Funder ID: 10.13039/501100001809).
- Zhejiang Provincial Natural Science Foundation of China (Grant No. LZ22E050006; Funder ID: 10.13039/501100004731).
- State Key Laboratory of Fluid Power and Mechatronic Systems (Grant No. SKLoFP_ZZ_2102; Funder ID: 10.13039/501100011310).
- The international cooperation program managed by the National Research Foundation of Korea (Grant Nos. 2021K2A9A2A06044278 and FY2021; Funder ID: 10.13039/501100003725).

Conflict of Interest

There are no conflicts of interest.

Data Availability Statement

To repeat and widely spread out the work in this paper, readers are welcome to use and update our codes available at the MathWorks File Exchange[2] and at the GitHub Repository[3]. Feedbacks are very much appreciated.

[2]https://ww2.mathworks.cn/matlabcentral/fileexchange/123480-surrogate-based-time-dependent-reliabillity-analysis

[3]https://github.com/WeifeiHuZJU/Surrogate-based-time-dependent-reliabillity-analysis

References

[1] Grieves, M. W., 2005, "Product Lifecycle Management: The New Paradigm for Enterprises," Int. J. Prod. Dev., **2**(1–2), pp. 71–84.

[2] Miller, A. M., Alvarez, R., and Hartman, N., 2018, "Towards an Extended Model-Based Definition for the Digital Twin," Comput. Aided Des. Appl., **15**(6), pp. 880–891.

[3] Tao, F., Sui, F., Liu, A., Qi, Q., Zhang, M., Song, B., Guo, Z., Lu, S. C.-Y., and Nee, A. Y., 2019, "Digital Twin-Driven Product Design Framework," Int. J. Prod. Res., **57**(12), pp. 3935–3953.

[4] Hu, W., He, Y., Liu, Z., Tan, J., Yang, M., and Chen, J., 2021, "Toward a Digital Twin: Time Series Prediction Based on a Hybrid Ensemble Empirical Mode Decomposition and BO-LSTM Neural Networks," ASME J. Mech. Des., **143**(5), p. 051705.

[5] Hu, W., Zhang, T., Deng, X., Liu, Z., and Tan, J., 2021, "Digital Twin: A State-of-the-art Review of its Enabling Technologies, Applications and Challenges," J. Intell. Manuf. Spec. Equip., **2**(1), pp. 1–34.

[6] Andrieu-Renaud, C., Sudret, B., and Lemaire, M., 2004, "The PHI2 Method: a way to Compute Time-Variant Reliability," Reliab. Eng. Syst. Saf., **84**(1), pp. 75–86.

[7] Sudret, B., 2008, "Analytical Derivation of the Outcrossing Rate in Time-Variant Reliability Problems," Struct. Infrastruct. Eng., **4**(5), pp. 353–362.

[8] Yang, J. N., and Shinozuka, M., 1972, "On the First-Excursion Probability in Stationary Narrow-Band Random Vibration, II," ASME J. Appl. Mech., **136**(3), pp. 765–785.

[9] Hu, Z., and Du, X., 2013, "Time-dependent Reliability Analysis with Joint Upcrossing Rates," Struct. Multidiscipl. Optim., **48**(5), pp. 893–907.

[10] Jiang, C., Wei, X. P., Huang, Z. L., and Liu, J., 2017, "An Outcrossing Rate Model and Its Efficient Calculation for Time-Dependent System Reliability Analysis," ASME J. Mech. Des., **139**(4), p. 041402.

[11] Romero, V. J., Swiler, L. P., and Giunta, A. A., 2004, "Construction of Response Surfaces Based on Progressive-Lattice-Sampling Experimental Designs with Application to Uncertainty Propagation," Struct. Saf., **26**(2), pp. 201–219.

[12] Zhao, W., Fan, F., and Wang, W., 2017, "Non-Linear Partial Least Squares Response Surface Method for Structural Reliability Analysis," Reliab. Eng. Syst. Saf., **161**, pp. 69–77.

[13] Blatman, G., and Sudret, B., 2010, "An Adaptive Algorithm to Build up Sparse Polynomial Chaos Expansions for Stochastic Finite Element Analysis," Probabilistic Eng. Mech., **25**(2), pp. 183–197.

[14] Dai, H., Zhang, H., Wang, W., and Xue, G., 2012, "Structural Reliability Assessment by Local Approximation of Limit State Functions Using Adaptive Markov Chain Simulation and Support Vector Regression," Comput.-Aided Civ. Infrastruct. Eng., **27**(9), pp. 676–686.

[15] Matheron, G., 1973, "The Intrinsic Random Functions and Their Applications," Adv. Appl. Probab., **5**(3), pp. 439–468.

[16] Wang, Z., and Wang, P., 2012, "A Nested Extreme Response Surface Approach for Time-Dependent Reliability-Based Design Optimization," ASME J. Mech. Des., **134**(12), p. 121007.

[17] Hu, Z., and Du, X., 2015, "Mixed Efficient Global Optimization for Time-Dependent Reliability Analysis," ASME J. Mech. Des., **137**(5), p. 051401.

[18] Li, J., Chen, J., and Fan, W., 2007, "The Equivalent Extreme-Value Event and Evaluation of the Structural System Reliability," Struct. Saf., **29**(2), pp. 112–131.

[19] Wang, Z., and Chen, W., 2017, "Confidence-Based Adaptive Extreme Response Surface for Time-Variant Reliability Analysis Under Random Excitation," Struct. Saf., **64**, pp. 76–86.

[20] Wu, H., Hu, Z., and Du, X., 2021, "Time-dependent System Reliability Analysis with Second-Order Reliability Method," ASME J. Mech. Des., **143**(3), p. 031101.

[21] Li, J., Chen, J., Wei, J., Zhang, X., and Han, B., 2019, "Developing an Instantaneous Response Surface Method t-IRS for Time-Dependent Reliability Analysis," Acta Mech. Solida Sin., **32**(4), pp. 446–462.

[22] Schleich, B., Anwer, N., Mathieu, L., and Wartzack, S., 2017, "Shaping the Digital Twin for Design and Production Engineering," CIRP Ann., **66**(1), pp. 141–144.

[23] Tuegel, E. J., Ingraffea, A. R., Eason, T. G., and Spottswood, S. M., 2011, "Reengineering Aircraft Structural Life Prediction Using a Digital Twin," Int. J. Aerosp. Eng., **2011**, p. 154798.

[24] Hu, W., Fang, J., Zhang, T., Liu, Z., and Tan, J., 2023, "A New Quantitative Digital Twin Maturity Model for High-End Equipment," J. Manuf. Syst., **66**, pp. 248–259.

[25] Echard, B., Gayton, N., and Lemaire, M., 2011, "AK-MCS: An Active Learning Reliability Method Combining Kriging and Monte Carlo Simulation," Struct. Saf., **33**(2), pp. 145–154.

[26] Xiao, S., Oladyshkin, S., and Nowak, W., 2020, "Reliability Analysis with Stratified Importance Sampling Based on Adaptive Kriging," Reliab. Eng. Syst. Saf., **197**, p. 106852.

[27] Yang, S., Jo, H., Lee, K., and Lee, I., 2022, "Expected System Improvement (ESI): A new Learning Function for System Reliability Analysis," Reliab. Eng. Syst. Saf., **222**, p. 108449.

[28] Jiang, C., Qiu, H., Yang, Z., Chen, L., Gao, L., and Li, P., 2019, "A General Failure-Pursuing Sampling Framework for Surrogate-Based Reliability Analysis," Reliab. Eng. Syst. Saf., **183**, pp. 47–59.

[29] Peng, X., Ye, T., Hu, W., Li, J., Liu, Z., and Jiang, S., 2022, "Construction of Adaptive Kriging Metamodel for Failure Probability Estimation Considering the Uncertainties of Distribution Parameters," Probabilistic Eng. Mech., **70**, p. 103353.

[30] Jiang, C., Qiu, H., Gao, L., Wang, D., Yang, Z., and Chen, L., 2020, "Real-time Estimation Error-Guided Active Learning Kriging Method for Time-Dependent Reliability Analysis," Appl. Math. Model., **77**, pp. 82–98.

[31] Song, Z., Zhang, H., Zhang, L., Liu, Z., and Zhu, P., 2022, "An Estimation Variance Reduction-Guided Adaptive Kriging Method for Efficient Time-Variant Structural Reliability Analysis," Mech. Syst. Signal Process., **178**, p. 109322.
[32] Li, C., and Der Kiureghian, A., 1993, "Optimal Discretization of Random Fields," J. Eng. Mech., **119**(6), pp. 1136–1154.
[33] Xu, S., Liu, H., Wang, X., and Jiang, X., 2014, "A Robust Error-Pursuing Sequential Sampling Approach for Global Metamodeling Based on Voronoi Diagram and Cross Validation," ASME J. Mech. Des., **136**(7), p. 071009.
[34] Aurenhammer, F., 1991, "Voronoi Diagrams—a Survey of a Fundamental Geometric Data Structure," ACM Comput. Surv., **23**(3), pp. 345–405.
[35] Crombecq, K., Gorissen, D., Deschrijver, D., and Dhaene, T., 2011, "A Novel Hybrid Sequential Design Strategy for Global Surrogate Modeling of Computer Experiments," SIAM J. Sci. Comput., **33**(4), pp. 1948–1974.
[36] Aute, V., Saleh, K., Abdelaziz, O., Azarm, S., and Radermacher, R., 2013, "Cross-Validation Based Single Response Adaptive Design of Experiments for Kriging Metamodeling of Deterministic Computer Simulations," Struct. Multidiscip. Optim., **48**(3), pp. 581–605.
[37] Bichon, B. J., Eldred, M. S., Swiler, L. P., Mahadevan, S., and McFarland, J. M., 2008, "Efficient Global Reliability Analysis for Nonlinear Implicit Performance Functions," AIAA J., **46**(10), pp. 2459–2468.
[38] Wang, Z., and Chen, W., 2016, "Time-variant Reliability Assessment Through Equivalent Stochastic Process Transformation," Reliab. Eng. Syst. Saf., **152**, pp. 166–175.
[39] Helton, J. C., and Davis, F. J., 2003, "Latin Hypercube Sampling and the Propagation of Uncertainty in Analyses of Complex Systems," Reliab. Eng. Syst. Saf., **81**(1), pp. 23–69.
[40] Zhang, D., Han, X., Jiang, C., Liu, J., and Li, Q., 2017, "Time-Dependent Reliability Analysis Through Response Surface Method," ASME J. Mech. Des., **139**(4), p. 041404.
[41] Chen, R., Liu, Y., Tan, L., and Zhou, B., 2012, "Research on Calculation of Thrust and Cutter Head Torque on Shield in Complex Strata," Chin. J. Undergr. Space Eng., **8**(1), pp. 26–32.